

THE MULTI-DIMENSIONAL ENSEMBLE EMPIRICAL MODE DECOMPOSITION METHOD

ZHAOHUA WU

*Department of Meteorology and
Center for Ocean-Atmospheric Prediction Studies
Florida State University
Tallahassee, FL 32306, USA*

NORDEN E. HUANG

*Research Center for Adaptive Data Analysis
National Central University
Chungli, Taiwan 32001, ROC*

XIANYAO CHEN

*The First Institute of Oceanography, SOA
Qingdao 266061, People's Republic of China*

A multi-dimensional ensemble empirical mode decomposition (MEEMD) for multi-dimensional data (such as images or solid with variable density) is proposed here. The decomposition is based on the applications of ensemble empirical mode decomposition (EEMD) to slices of data in each and every dimension involved. The final reconstruction of the corresponding intrinsic mode function (IMF) is based on a comparable minimal scale combination principle.

For two-dimensional spatial data or images, $f(x, y)$, we consider the data (or image) as a collection of one-dimensional series in both x -direction and y -direction. Each of the one-dimensional slices is decomposed through EEMD with the slice of the similar scale reconstructed in resulting two-dimensional pseudo-IMF-like components. This new two-dimensional data is further decomposed, but the data is considered as a collection of one-dimensional series in y -direction along locations in x -direction. In this way, we obtain a collection of two-dimensional components. These directly resulted components are further combined into a reduced set of final components based on a minimal-scale combination strategy.

The approach for two-dimensional spatial data can be extended to multi-dimensional data. EEMD is applied in the first dimension, then in the second direction, and then in the third direction, etc., using the almost identical procedure as for the two-dimensional spatial data. A similar comparable minimal-scale combination strategy can be applied to combine all the directly resulted components into a small set of multi-dimensional final components.

For multi-dimensional temporal-spatial data, EEMD is applied to time series of each spatial location to obtain IMF-like components of different time scales. All the i th IMF-like components of all the time series of all spatial locations are arranged to obtain i th temporal-spatial multi-dimensional IMF-like component. The same approach to the one used in temporal-spatial data decomposition is used to obtain the resulting

two-dimensional IMF-like components. This approach could be extended to any higher dimensional temporal-spatial data.

Keywords: Empirical mode decomposition (EMD); ensemble empirical mode decomposition (EEMD); minimal scale principle; pseudo multi-dimensional ensemble empirical mode decomposition; multi-dimensional ensemble empirical mode decomposition.

1. Introduction

The combination of empirical mode decomposition (EMD) with the Hilbert spectral analysis (HSA) designated as the Hilbert–Huang transform (HHT), in five patents^{1–5} by the National Aeronautics and Space Administration (NASA), has provided an alternative paradigm in time–frequency analysis. Though the Hilbert transform is well known and has been widely used in the signal processing field since 1940s,⁶ the Hilbert transform when applied for instantaneous frequency computation has many drawbacks^{7–10}; among them, the most serious one is its derived instantaneous frequency of a signal could lose its physical meaning when the signal is not a mono-component or AM/FM separable oscillatory function.^{9,10} The EMD, at its very beginning,^{9,11,12} was developed to overcome this drawback so that the data can be examined in a physically meaningful time–frequency–amplitude space. It has widely accepted that EMD, with its new improvements,^{10,13–18} has become a powerful tool in both signal processing and scientific data analysis.^{19–21}

Contrary to almost all the previous decomposition methods, EMD is empirical, intuitive, direct, and adaptive, without pre-determined basis functions. The decomposition is designed to seek the different simple intrinsic modes of oscillations in any data based on local time scales. A simple oscillatory mode is called intrinsic mode function (IMF) which satisfies: (a) in the whole data set, the number of extrema and the number of zero-crossings must either equal or differ at most by one; and (b) at any point, the mean value of the envelope defined by the local maxima and the envelope defined by the local minima is zero.

As described in Ref. 9, the EMD is implemented through a sifting process that uses only local extrema. From any data r_{j-1} , say, the procedure is as follows: (i) identify all the local extrema and connect all local maxima (minima) with a cubic spline as the upper (lower) envelope; (ii) obtain the first component h by taking the difference between the data and the local mean of the two envelopes; and (iii) treat h as the data and repeat steps (i) and (ii) until the envelopes are symmetric with respect to zero mean under certain criterion. The final h is designated as c_j . A complete sifting process stops when the residue, r_n , becomes a monotonic function or a function with only one extremum from which no more IMF can be extracted. In short, the EMD is an adaptive method that decompose data $x(t)$ in terms of IMFs c_j and a residual component r_n , i.e.,

$$x(t) = \sum_{j=1}^n c_j + r_n. \quad (1)$$

In Eq. (1), the residual component r_n could be a constant, a monotonic function, or a function containing only a single extrema, from which no more IMF can be extracted. In this way, the decomposition method is adaptive, and, therefore, highly efficient. As the decomposition is based on the local characteristics of the data, it is applicable to nonlinear and nonstationary processes.

Although EMD is a simple decomposition method, it has many intriguing but useful characteristics that other decomposition methods lack. Flandrin *et al.*²²⁻²⁴ studied the Fourier spectra of IMFs of fractional Gaussian noise, which are widely used in the signal processing community and financial data simulation. They found that the spectra of all IMFs except the first one of any fractional Gaussian noise collapse to a single shape along the axis of the logarithm of frequency (or period) with appropriate amplitude scaling of the spectra. The center frequencies (periods) of the spectra of the neighboring IMFs are approximately halved (and hence doubled); therefore, the EMD is essentially a dyadic filter bank. Flandrin *et al.*²³ also demonstrated that EMD behaves like a cubic spline wavelet when it is applied to Delta functions. Independently, Wu and Huang¹⁴⁻¹⁶ found the same result for white noise (which is a special case of fractional Gaussian noise). In addition to that, Wu and Huang^{14,15} argued using the central limit theorem that each IMF of Gaussian noise is approximately Gaussian distributed, and therefore, the energy of each IMF must be a X^2 distribution. From the characteristics they obtained, Wu and Huang^{14,15} further derived the expected energy distribution of IMFs of white noise. By determining the number of degrees of freedom of the X^2 distribution for each IMF of noise, they derived the analytic form of the spread function of the energy of IMF. From these results, one would be able to discriminate an IMF of data containing signals from that of only white noise with any arbitrary statistical significance level. They verified their analytic results with those from the Monte Carlo test and found consistency.

The power of EMD has stimulated the development of two-dimensional EMD (or bi-dimensional EMD, BEMD, as will be referred later). So far, many researchers have explored the possibility of extending EMD for multi-dimensional spatial-temporal data analysis. Mostly, the efforts succeeded only for spatial two-dimensional image analysis. The earliest trial of such efforts is to treat two-dimensional image as a collection of one-dimensional slices and then decompose each slice using one-dimensional EMD. This is a pseudo-two-dimensional EMD. The first attempt of such type was initiated by Huang.² This method was later used by Long²⁵ on wave data and produced excellent patterns and statistics of surface ripple riding on underlying long waves. In general, such an approach seems to work well in some cases of dealing with spatial data when a dominant direction could be identified clearly. However, in most of cases of pseudo-BEMD, the spatial structure is essentially determined by textual scales. If spatial structures of different textual scales are well distinguishable, with clear directionality and without intermittency, this approach would be appropriate. If it is not, the applicability of this approach is significantly reduced. The main shortcoming of this approach is the inter-slice

discontinuity due to EMD being sensitive to small data perturbation, intermittency, and highly variable directionality which we will discuss more in detail in Sec. 3.

The second type of effort is to directly transplant the idea and algorithm behind EMD to image decomposition. As it has been introduced early, while EMD is an one-dimensional data decomposition method, its essential step of fitting extrema of one-dimensional data with upper and lower curves (envelopes) using cubic spline or low order polynomials is applicable straightforwardly to two-dimensional images, with fitting surfaces replacing fitting curves. Currently, there are several versions of genuine two-dimensional EMD, each containing a fitting surface determined by its own method. Nunes *et al.*^{26–28} used a radial basis function for surface interpretation, and the Riesz transform rather than the Hilbert transform for computing the local wave number. Linderhed^{29,30} used the thin-plate spline for surface interpretation to develop two-dimensional EMD data for an image compression scheme, which has been demonstrated to retain a much higher degree of fidelity than any of the data compression schemes using various wavelet bases. Song and Zhang,³¹ Damerval *et al.*³² and Yuan *et al.*³³ used a method based on Delaunay triangulation and on piecewise cubic polynomial interpretation to obtain an upper surface and a lower surface. Xu *et al.*³⁴ provided still another approach by using a mesh fitting method based on finite elements. These BEMDs have accomplished some successes when they are applied to various fields of engineering and sciences. The advantages, computational cost, and the accuracy of different methods were studied and compared by Bhuiyan *et al.*³⁵ They concluded that the radial basis function using cubic and thin-plate splines, and Gaussian interpolations or inverse multi-quadric method could perform better than the other methods. Besides other difficulties to be discussed presently, the computation cost is still extremely high.

All the currently available traditional BEMDs, as those mentioned earlier, have several fundamental difficulties. The first one is the definition of extrema. All two-dimensional data have saddle, ridge, and trough structures, one need to make a decision of whether the saddle and ridge (trough) points should be considered maxima (minima). The fitting surfaces could be greatly different in the case of considering saddle and ridge (trough) points as maxima and in the case of not doing so. Consequently, the decomposition results would be dramatically different. The second difficulty is the surface fitting can be computationally expensive. In many cases, it involves very large matrix and its eigenvalue computations, and the fittings offer only an approximation and could not go through all the actual extrema. The third difficulty, and probably the most serious one, is the mode mixing, or more generally, scale mixing. In one-dimensional EMD, scale mixing is defined as a single IMF either consisting of signals of widely disparate scales, or a signal of a similar scale residing in different IMF components, caused by unevenly distributed extrema along the time axis.^{5,12,16} This concept of scale mixing can be easily extended to BEMD. Let us consider this example: given a data consisted of two-dimensional sinusoidal waves. If the data is contaminated by noise only in the lower-left quarter of the image, the scale of the noise is widely distributed in comparison with the sinusoidal

wave. Therefore, the decomposition will mix the noise scale with the sinusoidal wave that could lead to the decomposed components in the contaminated area having no two-dimensional sinusoidal wave, while the rest of the area still covered with the original sinusoidal wave. Since all data contain noise, such decomposition using BEMD is unstable and can be very sensitive to noise, essentially leading to the physically uninterpretable results, similar to the one-dimensional case described by Huang *et al.*¹² and Wu and Huang.^{5,16}

In this paper, we will introduce a new multi-dimensional EMD method based on the ensemble EMD (EEMD^{5,16}), a noise assisted data analysis method that overcomes many drawbacks of EMD such as the sensitivity of decomposition to small perturbation of data. It will be demonstrated that, with good properties of EEMD, the inter-slice discontinuity existed in pseudo-BEMD is no longer a daunting problem. By applying EEMD to spatial data in one dimension (pseudo-BEMD) and then followed by applying EEMD in the second dimension to the results of the decompositions of the first dimension, and then applying a new strategy of combining of appropriate components, we obtain the decompositions of image. It will be shown that this EEMD-based bi-dimensional approach can be extended to spatial data of any number of dimensions. In Sec. 2, the effects of EEMD in the present application will be discussed. Section 3 will discuss the improvement of the pseudo-BEMD with the usage of EEMD. Section 4 will discuss EEMD based BEMD and its extension for the decomposition of multi-dimensional spatial data. Section 5 will provide extra examples from various fields of science and engineering. The summary and discussion will be presented in Sec. 6.

2. Ensemble Empirical Mode Decomposition

As mentioned earlier, one of the major drawbacks of EMD is mode mixing, which is defined as a single IMF either consisting of signals of widely disparate scales, or a signal of a similar scale residing in different IMF components. Mode mixing is a consequence of signal intermittency. As discussed by Huang *et al.*,^{9,12} the intermittency could not only cause serious aliasing in the time–frequency distribution, but also make the individual IMF lose its clear physical meaning. Another side-effect of mode mixing is the lack of physical uniqueness. An illustrative example is decompositions of two time series corresponding to the observations of sea surface temperature (SST) which differ slightly at any time. Due to scale mixing, the decompositions could be significantly different, which is shown in Fig. 1.

Clearly, in this example, all corresponding components around 1960 and 1970 are significantly different. There are significant differences in decomposed IMF but only minor differences in the original inputs raises a question: which decomposition is reliable?

The answer to this question can never be definite. However, since the cause of the problem is due to mode (scale) mixing, one expects that the decomposition would be reliable if the mode mixing problem is alleviated or eliminated. To achieve the latter

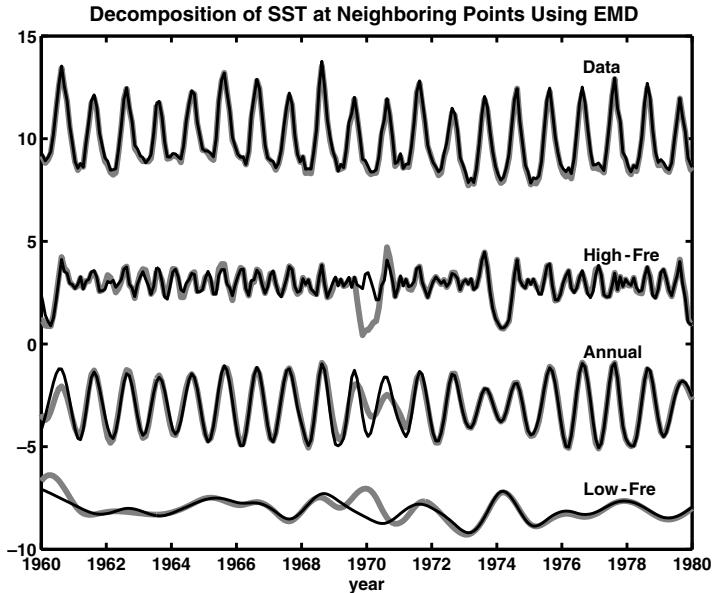


Fig. 1. The mode (scale) mixing and the sensitivity of decomposition of the empirical mode decomposition to small perturbation. The data of two SST observations³⁶ of spatial locations (20°W , 60°N) and (19°W , 60°N) are plotted as the bold gray and thin black lines, respectively. Their corresponding components are also plotted as the bold gray and thin black lines, respectively. The numbers in the vertical scales provide the scales of variability of both observations and their components.

goal, Huang *et al.*¹⁰ proposed an intermittency test. However, the approach itself has its own problems: first, the test is based on a subjectively selected scale, which makes EMD no longer totally adaptive. Second, the subjective selection of scales may not work if the scales are not clearly separable. To overcome the scale mixing problem, a new noise-assisted data analysis method was proposed, the ensemble EMD (EEMD^{5,16}), which defines the IMF components as the mean of an ensemble, each consisting of the signal plus a white noise of finite amplitude. The true IMF should be the result when the number of the ensemble approach to infinity.

Ensemble EMD is also an algorithm, which contains the following steps:

- (a) add a white noise series to the targeted data;
- (b) decompose the data with added white noise into IMFs;
- (c) repeat step (a) and step (b) again and again, but with different white noise series each time; and
- (d) obtain the (ensemble) means of corresponding IMFs of the decompositions as the final result.

The principle of EEMD is simple: the added white noise would populate the whole time–frequency space uniformly with the constituting components at different scales. When the signal is added to this uniform background, the bits of signals of

different scales are automatically projected onto proper scales of reference established by the white noise. Although each individual trial may produce very noisy results, the noise in each trial is canceled out in the ensemble mean of enough trails; the ensemble mean is treated as the true answer when the trials in the ensemble approach to infinity. In practice, we could select a large enough trial number as long as we could tolerate the residue of the contamination from the added noise.

The critical concepts advanced in EEMD are based on the following observations:

- (i) A collection of white noise cancels each other out in a time space ensemble mean; therefore, only the signal can survive and persist in the final noise-added signal ensemble mean.
- (ii) Finite, not infinitesimal, amplitude white noise is necessary to force the ensemble to exhaust all possible solutions; the finite magnitude noise makes the different scale signals reside in the corresponding IMFs, dictated by the dyadic filter banks, and render the resulting ensemble mean more meaningful.
- (iii) The physically meaningful answer of the EMD is not the one without noise; it is designated to be the ensemble mean of a large number of trials consisting of the noise-added signal.

As an analogue to a physical experiment that could be repeated many times, the added white noise is treated as the possible random noise that would be encountered in the measurement process. Under such conditions, the i th “artificial” observation will be

$$x_i(t) = x(t) + w_i(t), \quad (2)$$

where $w_i(t)$ is the i th realization of the white noise series. In this way, multiple artificial observations are mimicked.

As the ensemble number approaches infinity, the truth, $c_j(t)$, as defined by EEMD, is

$$c_j(t) = \lim_{N \rightarrow \infty} \frac{1}{N} \sum_{k=1}^N [c_j(t) + r_k(t)], \quad (3)$$

in which

$$c_j(t) + r_k(t) \quad (4)$$

is the k th trial of the j th IMF in the noise-added signal. The amplitude of noise $w_i(t)$ is not necessarily small. But the ensemble number of the trials, N , has to be large. The difference between the truth and the result of the ensemble is governed by the well-known statistical rule: it decreases as one over the square-root of N .^{5,16}

With EEMD, the mode mixing is largely eliminated and the consistency of the decompositions of slightly different pairs of data, as given in the example illustrated in Fig. 1, are greatly improved, as illustrated in Fig. 2. Indeed, EEMD represents a major improvement over the original EMD. As the level of added noise is not of

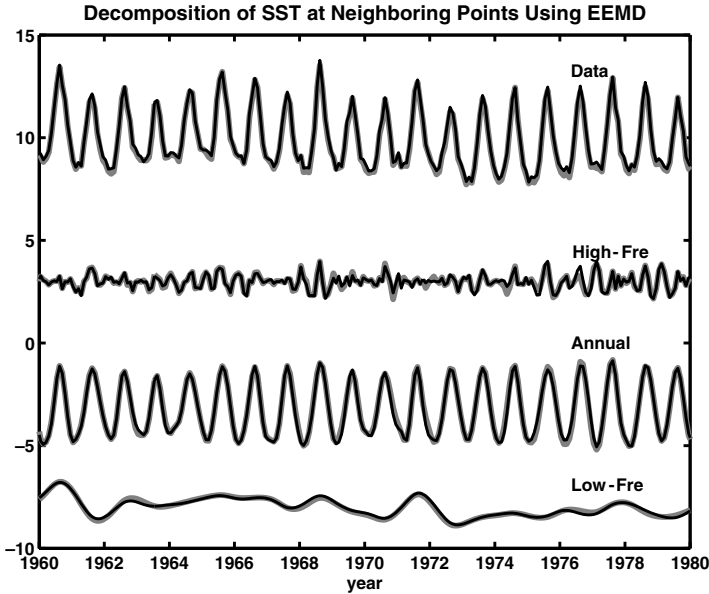


Fig. 2. Same data as given in Fig. 1, but analyzed with ensemble empirical mode decomposition replacing empirical mode decomposition.

critical importance, as long as it is of finite amplitude while allowing for a fair and large number of ensemble of all the possibilities. EEMD can be used without any significant subjective intervention; thus, it provides a truly adaptive data analysis method. By eliminating the problem of mode mixing, it also produces a set of IMFs that may bear the full physical meaning for each IMF component, and a time–frequency distribution without transitional gaps. The EMD, with the ensemble approach, has become a more mature tool for nonlinear and nonstationary time series (and other one-dimensional data) analysis.

The EEMD resolves, to a large degree, the problem of mode mixing.^{12,13} It might have resolved the physical uniqueness problem too, for the finite magnitude perturbations introduced by the added noises have produced the mean in the neighborhood of all possibilities.

3. Pseudo-Bi-Dimensional Empirical Mode Decomposition

The pseudo-BEMD that was used in Refs. 2 and 25 is as the following: suppose that we have a temporal-spatial field $f(\vec{s}, t)$ with M spatial locations and each having N temporal records

$$f(m, n) = \begin{pmatrix} f_{1,1} & f_{2,1} & \cdots & f_{M,1} \\ f_{1,2} & f_{2,2} & \cdots & f_{M,2} \\ \cdots & \cdots & \cdots & \cdots \\ f_{1,N} & f_{2,N} & \cdots & f_{M,N} \end{pmatrix}, \tag{5}$$

in which each column is a time series of the evolution of a quantity at a spatial location. We write m th column of the gridded data as

$$f(m, \sim) = \begin{pmatrix} f_{m,1} \\ f_{m,2} \\ \dots \\ f_{m,N} \end{pmatrix}. \quad (6)$$

Its decompositions using EMD is

$$f(m, \sim) = \sum_{j=1}^J C_j(m, \sim) = \sum_{j=1}^J \begin{pmatrix} c_{m,1,j} \\ c_{m,2,j} \\ \dots \\ c_{m,N,j} \end{pmatrix}. \quad (7)$$

After all columns of the original data are decomposed, we rearrange the outputs into J number of matrices, with j th matrix being

$$g_j(m, n) = \begin{pmatrix} c_{1,1,j} & c_{2,1,j} & \dots & c_{M,1,j} \\ c_{1,2,j} & c_{2,2,j} & \dots & c_{M,2,j} \\ \dots & \dots & \dots & \dots \\ c_{1,N,j} & c_{2,N,j} & \dots & c_{M,N,j} \end{pmatrix}. \quad (8)$$

In this way, we obtain J components of the original data $f(m, n)$. Due to the scale mixing problem of EMD as described in the previous section, the inter-slice discontinuity could be very severe. Let us consider the example as shown in Fig. 3, in which the decomposition of the observed SST from 30°W to 10°W along 60°N is plotted. Clearly, there are unorganized scattered large values in all the components in Fig. 3 which are harder to be interpreted physically. But, as the noise magnitude is limited and small compared with the signal. Furthermore, the distribution of the noise is random; the over all quality of the image is still smooth and the pattern reasonable. If one used EMD along each linear segment of the data, the resulting image constituted from the decomposed components would have totally distorted features and devoid of any discernable pattern and physical meaning.

Since EEMD eliminates largely the scale mixing problem and preserves physical uniqueness of the components, with EEMD replacing EMD, the contribution of the noises are distributed to the separate component according to their scales. As a result, the coherent structures of the components emerge, as shown in Fig. 4. In this way, the pseudo-BEMD method can be applied to reveal the evolution of spatial structures of data.

It should be pointed out here that the “pseudo-BEMD” method is not limited to only one-spatial dimension; rather, it can be applied to data of any number of spatial-temporal dimensions. Since the spatial structure is essentially determined by timescales of the variability of a physical quantity at each location and the decomposition is completely based on the characteristics of individual time series at each spatial location, there is no *a priori* assumption of spatial coherent structures

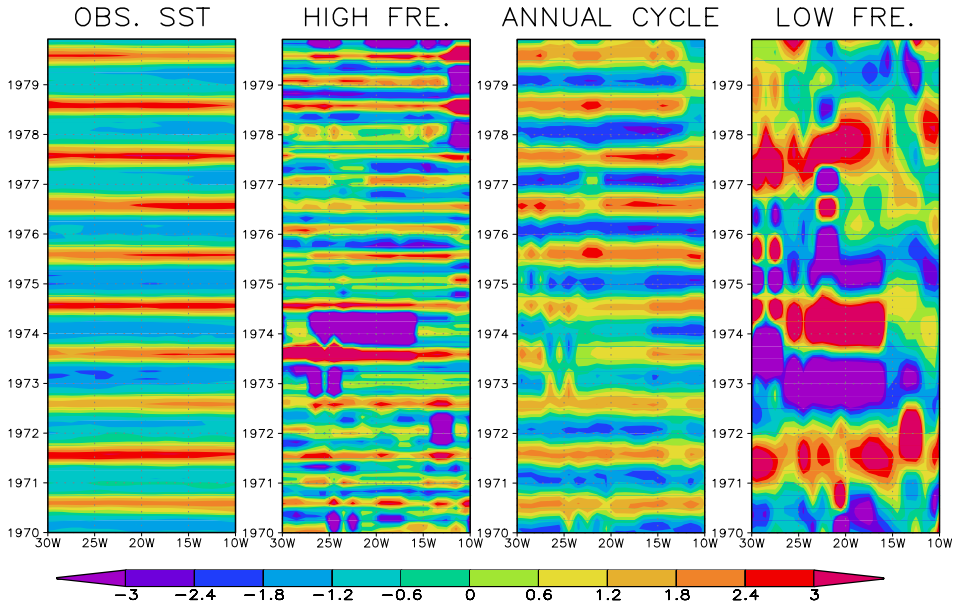


Fig. 3. Decomposition of the sea surface temperature (SST) from 30°W to 10°W along 60°N latitude using EMD-based pseudo-BEMD. Panels from the left to the right are the SST, its high-frequency component, its MAC, and its low-frequency component. The color bar provides the shaded interval for the left panel. For the panels 2–4 from the left, the shaded interval should be the color bar multiplied by a factor of 1/3, 5/6, and 1/6, respectively.

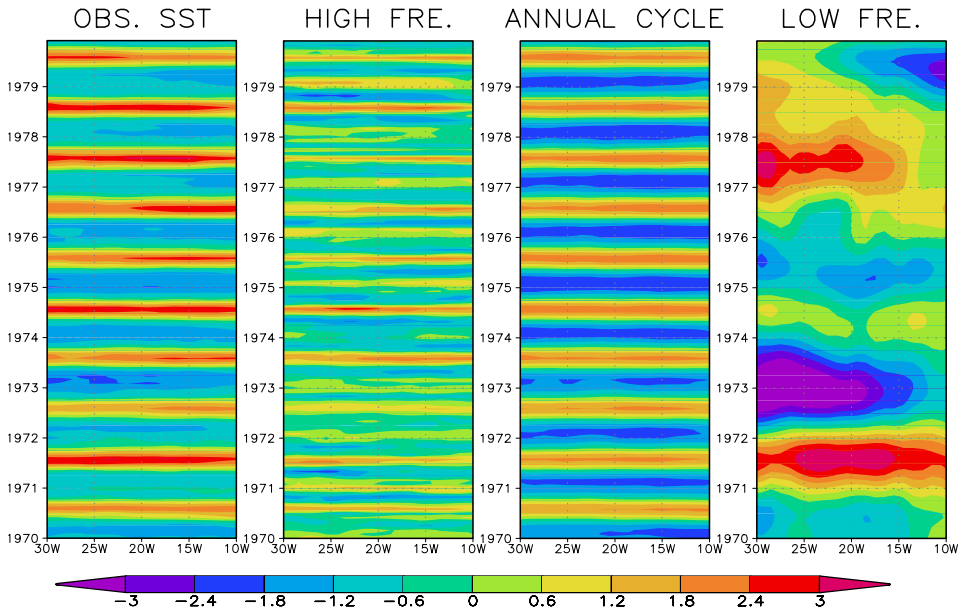


Fig. 4. The same as in Fig. 3, but with EEMD-based pseudo-BEMD replacing EMD-based pseudo-BEMD.

of this physical quantity. When a coherent spatial structure emerges, it reflects better the physical processes that drive the evolution of the physical quantity on the timescale of each component. Therefore, we expect this method to have significant applications in spatial-temporal data analysis.

4. EEMD-Based Two-Dimensional Empirical Model Decomposition

As we mentioned in the introduction, the traditional BEMD has several daunting difficulties. To overcome these difficulties, the application of EEMD idea to the traditional BEMD is theoretically feasible: (i) perturbing original spatially two-dimensional data with different realizations of white noise; (ii) decomposing the noise-perturbed data using one of the traditional BEMD method; and (iii) taking the ensemble mean of the corresponding BEMD products. Although such an ensemble BEMD approach is straightforward and can eliminate the difficulties in defining extrema in spatially two-dimensional data and the problem of scale mixing as in one-dimensional cases, the ensemble approach requires larger computational resource that is linearly proportional to the number of the ensemble trials as the regular BEMD. A typical implementation of EEMD is usually 100 independent trials in the ensemble, the computation cost would be prohibitive. This large demand of computational resource by far has imposed a barrier of developing ensemble BEMD. In Sec. 3, it is demonstrated that inter-sliced discontinuity in pseudo-BEMD using traditional EMD can be eliminated by replacing EMD with EEMD. However, for most of two-dimensional data or images that are to be decomposed and analyzed, we do not have the luxury of having a coherence structure associated with the spatial scales in a particular direction such as in the case of temporal-spatial data. Therefore, other than the special example given above in Figs. 3 and 4, the temporal-spatial pseudo-BEMD is often not successful to analyze or decompose spatially two-dimensional data or images. These existing deficiencies of the current BEMD methods (including the pseudo approaches) have forced us to search an alternative adaptive two-dimensional data decomposition method to the traditional BEMD for practical use.

4.1. Decomposition of two-dimensional data using EEMD

As shown in Secs. 2 and 3, the EEMD is a spatial-temporally local filtering method dictated by dyadic filter windows while still keeps its adaptive nature; therefore, it can allocate variability of two-dimensional data into appropriate components of certain timescales. Since spatial two-dimensional data or images usually do not have preferred structure in a given direction (otherwise, the two-dimensional data or images are degenerated to one-dimension data), the data or images should be equally treated in any given orthogonal directions. Therefore, the one-dimensional decomposition such as in pseudo-BEMD is not enough; and decomposition must be performed in two orthogonal directions. Suppose now $f(m, n)$ in Eq. (5) represents

spatially two-dimensional data or an image $f(x, y)$, after it is decomposed in one-direction, suppose y -direction, we obtain components $g_j(m, n)$ as expressed in Eq. (8), we further decompose each row of $g_j(m, n)$ using EEMD as done in previous section. The details are given as follows:

For convenience, we write the n th row of j th component $g_j(\sim, n)$ of $f(m, n)$ and its EEMD decomposition as,

$$g_j(\sim, n) = (c_{1,n,j} \quad c_{2,n,j} \quad \cdots \quad c_{M,n,j}), \quad (9)$$

and

$$g_j(\sim, n) = \sum_{k=1}^K D_{j,k}(\sim, n) = \sum_{k=1}^K (d_{1,n,j,k} \quad d_{2,n,j,k} \quad \cdots \quad d_{M,n,j,k}), \quad (10)$$

respectively. Similar to the pseudo-BEMD case, we rearrange the decomposition component as

$$h_{j,k}(m, n) = \begin{pmatrix} d_{1,1,j,k} & d_{2,1,j,k} & \cdots & d_{M,1,j,k} \\ d_{1,2,j,k} & d_{2,2,j,k} & \cdots & d_{M,2,j,k} \\ \cdots & \cdots & \cdots & \cdots \\ d_{1,N,j,k} & d_{2,N,j,k} & \cdots & d_{M,N,j,k} \end{pmatrix}. \quad (11)$$

The complete decomposition is

$$f(m, n) = \sum_{k=1}^K \sum_{j=1}^J h_{j,k}(m, n). \quad (12)$$

An example of such decomposition is given in Figs. 5 and 6, with Fig. 5 displaying the original data (with a size of horizontal and vertical grid points of 97 each) which is the numerically simulated vertical velocity at 500 hPa level (around the mid of the troposphere) of hurricane Andrew of 1992, and Fig. 6 displaying its components obtained by using EEMD on each slice in both directions. The top row represents the decomposition in the horizontal direction; each image is decomposed in the vertical direction with their results displayed in the vertical columns.

4.2. Strategy of combining components

The results shown in Fig. 6 do not provide important information about the convection structure of the hurricane Andrew. The structure of each component shows orientation (combination of different spatial scales in different directions), for example, the zero lines of $h_{1,5}$ are almost all vertically oriented while those of $h_{5,1}$ are all horizontally oriented. This makes us to wonder that such a BEMD in two orthogonal directions are useful to reveal important information of an image of a physical system.

To proceed, we make a detour to consider what is the most important capability of a two-dimensional decomposition method. Suppose we have a line drawing of a

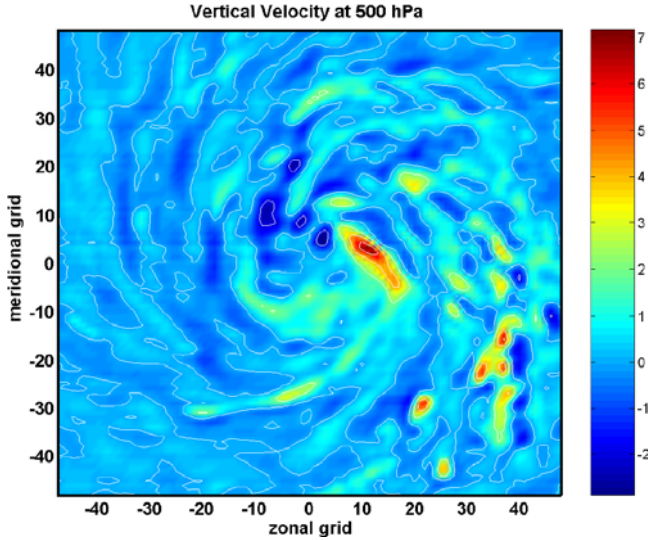


Fig. 5. The numerically simulated vertical velocity at 500 hPa level of Hurricane Rita of 2005. The warm color represents the upward motion and the cold color downward motion. The unit is m/s.

rectangle as displayed in Fig. 7. When it is decomposed using a two-dimensional decomposition method, the ideal solution should be that one of the IMF components captures the whole rectangle. Clearly the rectangle has several spatial scales: the small spatial scale of line thickness, and the large spatial scales of the lengths of the different sides. When EEMD is applied to the horizontal and vertical directions separately as described in Sec. 4.1, the decomposition results in components are incapable of capturing the whole rectangle in any one component, since EEMD is, in principle, a dyadic filter. However, one of these components that have horizontal scales of about line thickness and vertical scales of about the length of the vertical line captures the two vertical lines of the rectangle. Similarly, one of these components captures the two horizontal lines of the rectangle. The combination of these two components should capture the whole rectangle. Clearly, the common feature of these two components is that their minimal scales are the line thickness, the minimal spatial scales of each of these two components.

With the above discussion in mind, our EEMD-based BEMD involves a new combination strategy, the comparable minimal scale combination principle: *among all the components resulted from applying of EEMD in two orthogonal directions, the combination of the components having comparable minimal scales would give the most meaningful results. This combination will give a single IMF component revealing the true two-dimensional feature of the data.*

The above statement seems to require the examination of the minimal scales of each component resulted from the decomposition in Sec. 4.1. In reality, it is not! With the way the order of the decomposition using EEMD is carried out, such as the

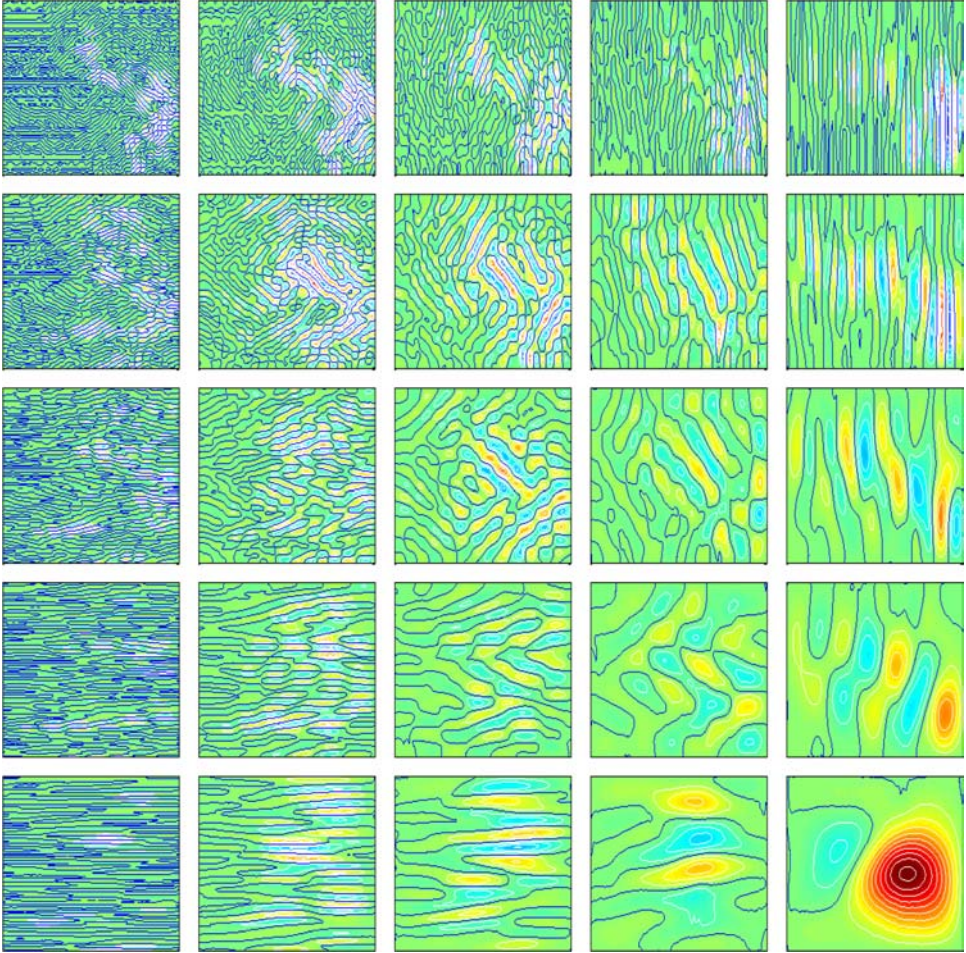


Fig. 6. The EEMD components of the vertical velocity displayed in Fig. 5. In each panel, the color scales are different, the blue lines correspond to zeros.

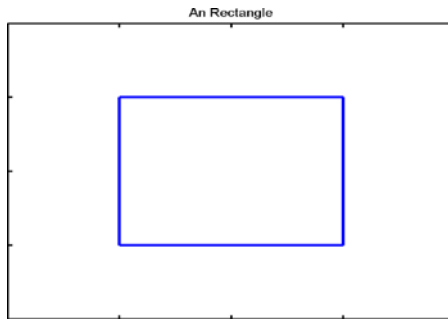


Fig. 7. A rectangle.

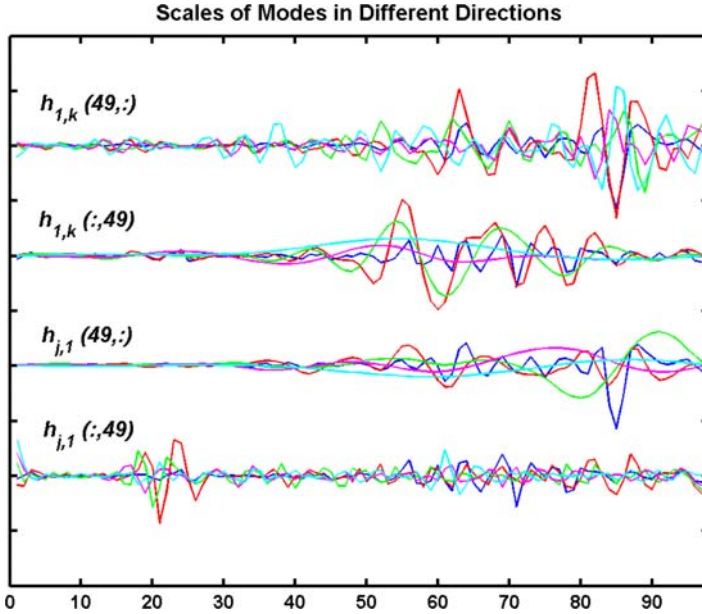


Fig. 8. The vertical velocity oscillations of the first row components and the first column components along the central vertical lines and horizontal lines of each row. The first (second) group (from the top) of the lines are the velocity oscillations of the first row of components (displayed in Fig. 6) along the middle horizontal (vertical) line of each component; and the third (fourth) group (from the top) of the lines are the velocity oscillations of the first column of components (displayed in Fig. 6) along the middle horizontal (vertical) line of each component. In the figure, the different color of lines correspond to different panels, with blue lines corresponding to i or j equal to 1, red lines 2; green lines 3, magenta lines 4, and cyan lines 5.

components displayed in Fig. 6, each row of components would have approximately the same horizontal scale and each column approximately the same vertical scale. Such a property can be easily verified. In Fig. 8, we display the vertical velocity oscillations of the first row components and the first column components along the central vertical lines and horizontal lines of each row, the 49th line out of 97 total data lines in each direction. While the details of each line are different, the minimal spatial scales (in the horizontal direction) of the first row $h_{1,k}$ and the minimal spatial scales (in the vertical direction) of the first column $h_{j,1}$ of the components are approximately the same, although the vertical (horizontal) scales of the first row (column) increase as k (j) increase.

In light of the above results and discussions, the combination of modes can be very simple: the final i th component C_i of the decomposition can be written as

$$C_i = \sum_{k=i}^K h_{i,k} + \sum_{j=i+1}^J h_{j,i}, \tag{13}$$

which is displayed in Table 1.

Table 1. The visual schematic of the combinations of components resulted from applying EEMD to data in two orthogonal directions for the case of $J = K$, as expressed by Eq. (11). The components listed in the neighboring cells with the same shade are summed to form a final mode. The final components are expressed in Eq. (11).

$h_{1,1}$	$h_{1,2}$...	$h_{1,K}$
$h_{2,1}$	$h_{2,2}$...	$h_{2,K}$
...
$h_{K,1}$	$h_{K,2}$...	$h_{K,K}$

The final components of the hurricane Andrew is displayed in Fig. 9. The decomposition reveals interesting features of the hurricane Andrew, such as mass sucked in by the hurricane vortex, gravity waves, and vortex Rossby waves. The first component represents the finest structure that is not seen by directly viewing the original vertical velocity field; and the second component catches the general impression of the original vertical velocity field. Both components display the suck-in structure of the vortex, and are consistent with the sweeping rain bands (corresponding to the upward motion bands) of the hurricane. Indeed, the results are very similar to the regression of radar reflection signals of Andrew. Component 3 is associated with gravity waves, and components 4 and 5 (the remainder) are associated with large scale waves (Rossby waves) that are not seen in the original wind field. These waves are polarized along the hurricane track, indicating that these waves may be important in determining the track of the hurricane, and can potentially provide some prediction skills for hurricane track.

It should be pointed out that the results displayed in Fig. 9 are not sensitive to either the north–south direction (the vertical direction displayed in previous figures) or the east–west direction (the horizontal direction). The vortex-type structure of the hurricane and its final structure essentially imply that the decomposition is independent of the selection of the orthogonal reference frame for the decomposition as long as same grid distance with respect to the orthogonal reference frame is selected.

4.3. *Extension to multi-dimension decomposition*

The decomposition scheme proposed here could be extended to data of any multi-dimension such as data of a solid with different density or other measurable properties given as

$$I = f(x_1, x_2, \dots, x_n). \quad (14)$$

In which the subscription, n , indicated the number of dimensions. The procedure is identical as stated above: the decomposition starts with the first dimension,

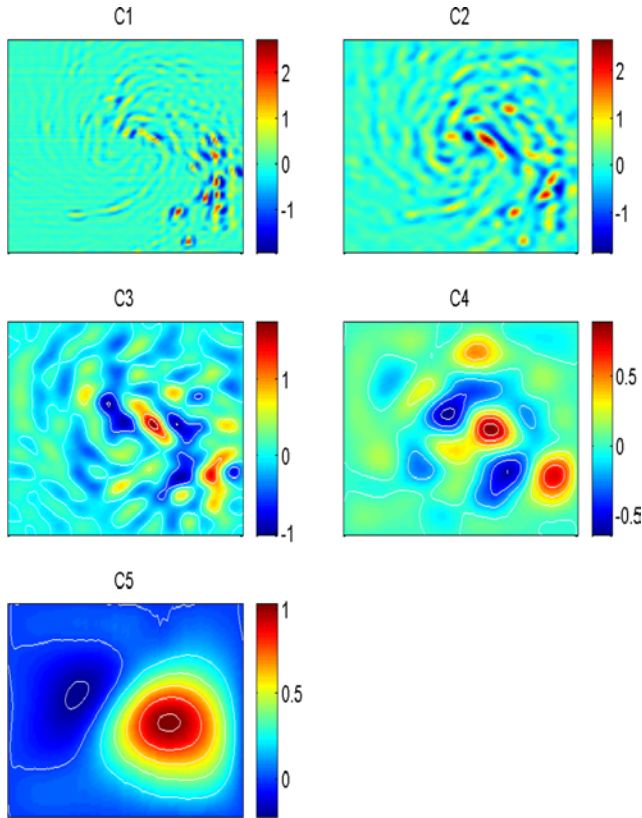


Fig. 9. The final IMF components of hurricane Andrew.

and proceeds to the second and third till all the dimensions are exhausted. The decomposition is still implemented by slices. The schematic of reconstruction for a three-dimensional data is given in Fig. 10. It should be note that there is no difficulty in implementing this scheme, for the data analysis that consisted essentially of one-dimensional ensemble EMD.

This new approach is based on separating the original data into one-dimensional slices, then applying ensemble EMD to each one-dimensional slice. The key part of the method is in the construction of the IMF according to the principle of combination of the comparable minimal scale components. This method is designated as a multi-dimensional ensemble empirical mode decomposition (MEEMD).

5. MEEMD Examples

In the following, we will present some examples of the application of MEEMD to various types of data. The advantages of the method will be demonstrated through these examples.

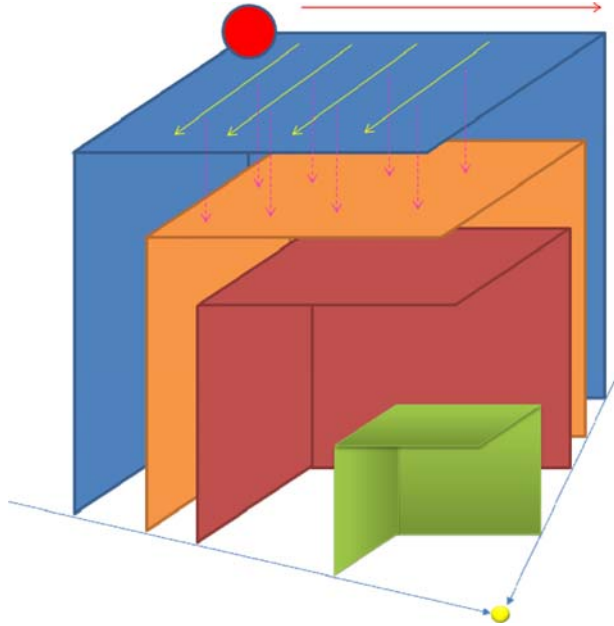


Fig. 10. Schematics of decomposition and reconstruction of multi-dimension EEMD. Large red point and small yellow point denote the original data (3D) and final IMFs, respectively. The red, yellow, and magenta arrows denote the first, second, and third decompose direction, respectively. The minimum scale combinations are taken along the three planes with the same color.

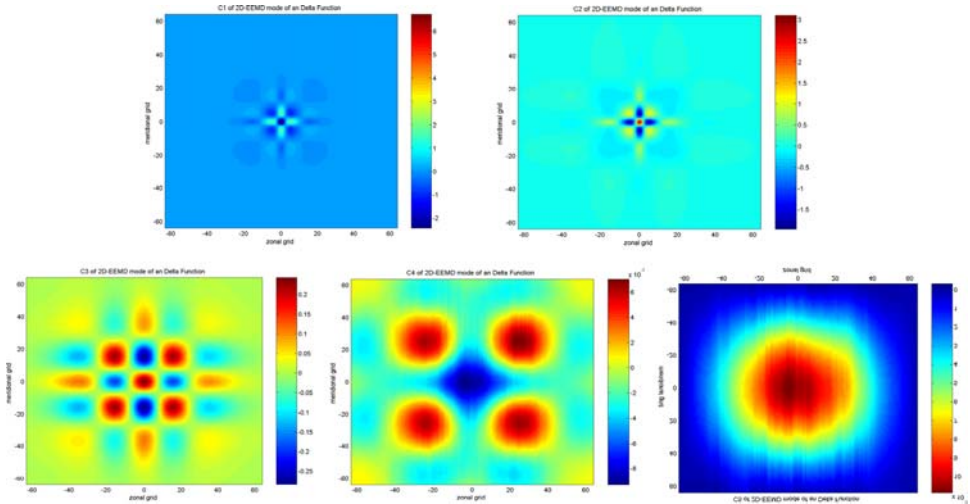


Fig. 11. The decomposition of a point source $[\delta(x, y)$ function] using 2D EMD.

5.1. Decomposition of a delta function

In this case, a delta function $\delta(x, y)$ is specified. The function has values zero at all grids except the origin, where the value is specified as 10. As shown in Fig. 11, the decomposition is not circularly symmetric with respect to the origin, and is similar to the decomposition of the same function using 2D directional wavelet decomposition. This orientation-sensitive result seems to contradict our assertion that the new MEEMD is orientation independent. However, the reason for this orientation-sensitive result is due to the fact that the delta function does not have any extrema except at the origin, which, in some sense, should not be considered a true two-dimensional field. If we consider the delta function as an average of many cases of noise perturbed delta functions, i.e.,

$$\delta(x, y) = \lim_{N \rightarrow \infty} \frac{1}{N} [\delta(x, y) + w_n(x, y)], \quad (15)$$

where $n = 1, \dots, N$, and $w_i(x, y)$ is one realization of two-dimensional Gaussian white noise of amplitude of the same order of the delta function, then by decomposing

$$\delta(x, y) + w_n(x, y) \quad (16)$$

using MEEMD and carrying out the average action to corresponding components (suppose all the components of the same rank) dictated by the dyadic filter property of EEMD, the resulted components show the circular structure. In this way, the apparent contradiction can be resolved.

There is a major improvement over the 2D directional wavelet decomposition. When the delta function like signal is moved around, the decomposition using MEEMD will give almost identical results except that all the components will be centered at the nonzero location of the delta function like signal. When 2D directional wavelet decomposition is applied, the components will have significantly different structures when the valued location of the delta function-like signal moves, a result of the lack of the locality and the adaptivity of the wavelet tools. This result can be easily verified.

5.2. Decomposition of a noise contaminated 2D signal

In this case, a two-dimensional synthetic data is decomposed using our approach to illustrate the capability of our new method in de-noising. The synthetic data is

$$\sin\left(\frac{\pi x}{24}\right) \sin\left(\frac{\pi y}{24}\right) + w(x, y),$$

where $w(x, y)$ is uniformly distributed noise with a value from 0 to 1.

The original signal and the decomposition are shown in Fig. 12. The extracted noise field is very similar to the specified noise field, with a correlation coefficient

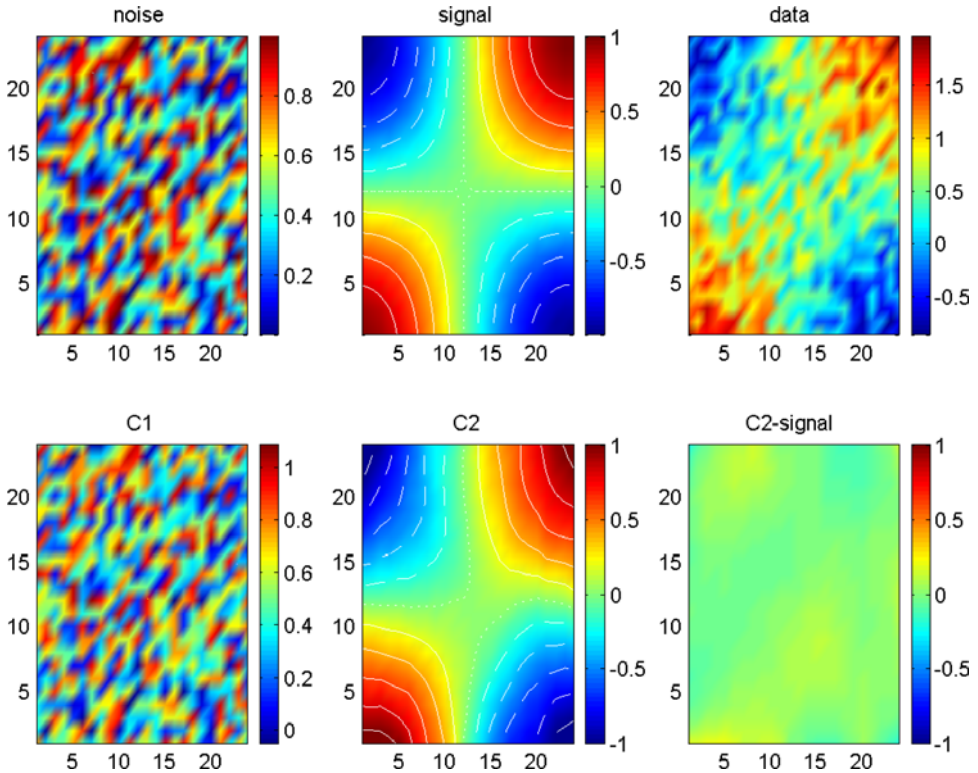


Fig. 12. Decomposition of a noise contaminated two-dimensional signal. Upper left panel: the noise N ; upper middle panel: the specified signal (S); upper right panel: the synthetic noise contaminated 2D signal ($S + N$); lower left panel: the sum of the decomposed small scale components (extracted noise, N'); lower middle panel: the sum of the decomposed large scale components (extracted signal, S'); and lower right panel: the difference between true signal (S) and the extracted signal (S').

over 0.95. Since the specified noise contains large-scale structure and the limited number of IMFs extracted noise could not contain all the different scales in the noise, the extracted signal is not exactly the specified original signal. However, this is not a drawback of the present approach, for the large scale signal contained noise is not distinguishable from the large scale signals. In general, the decomposition recovers very well the specified signal. In this sense, this method can be used to extracted 2D noise in various applications such as to clean up the speckles in medical ultra-sonic images, or enhance scanned images.

5.3. *Decomposition of Lena*

The third example is the decomposition of famous, or may be overly used image, Lena. Lena has been a popular image in the image processing fields, and has served as the bench-mark image for testing various methods. Our decomposition



Fig. 13. The decomposition of Lena (128×128 pixels). The upper panels are the original picture and the remainder after n components are extracted, $n = 1, 2, 3, 4$. The lower panels are 2D IMF components 1–4, from finer to large scale.

is displayed in Fig. 13, and its Matlab code (a scripting code) is provided in Appendix.

Careful examination of the decomposition will lead to the conclusion that the new MEEMD decomposition is superior to those using the other methods, including some traditional genuine 2D EMD method. The most important improvement is the elimination of scale mixing that happens in other 2D methods while still keeping the adaptivity. The first component is simply a line drawing of Lena, with sharp edges of the lines. The second component provides a blurred version of Lena. The combination of these two gives back the sharp version of the original image.

Another major improvement is the elimination of the artificial structure in the large scale. When scale mixing happened, it is a common occurrence that a relatively high positive value at a certain location in one component accompanying with a relatively high negative value at the same location in its neighboring components. Such paired structures are artificial. In early decomposition using other 2D EMD methods, e.g. in Refs. 29 and 30, such paired structure is extremely obvious in the large scale components. However, with the elimination of the scale mixing using our technique, the artificial structure is gone.

5.4. *Decomposition of medical image*

The fourth example is a medical application as described in Refs. 2–4. The image for this example is extracted from the Website of Harvard Medical School for Radiology at <http://www.med.harvard.edu/AANLIB/cases/case1/mr1-t14/029.html> with the images Fig. 14.

Clinically, the Harvard Website describes this case as: “A 51 year old woman sought medical attention because of gradually increasing right hemiparesis (weakness) and hemianopia (visual loss). At craniotomy (8/90), left parietal

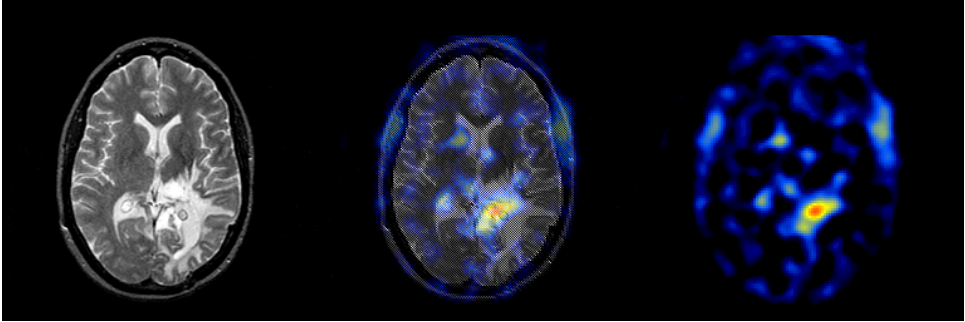


Fig. 14. The images given above show the T2-weighted MR (left), Thallium SPECT (right), and their overlay (central). The red-and-yellow bright-hot area in the Thallium SPECT represents the active tumor lesion. Note the Thallium SPECT does not cover all the abnormality area in MR image.

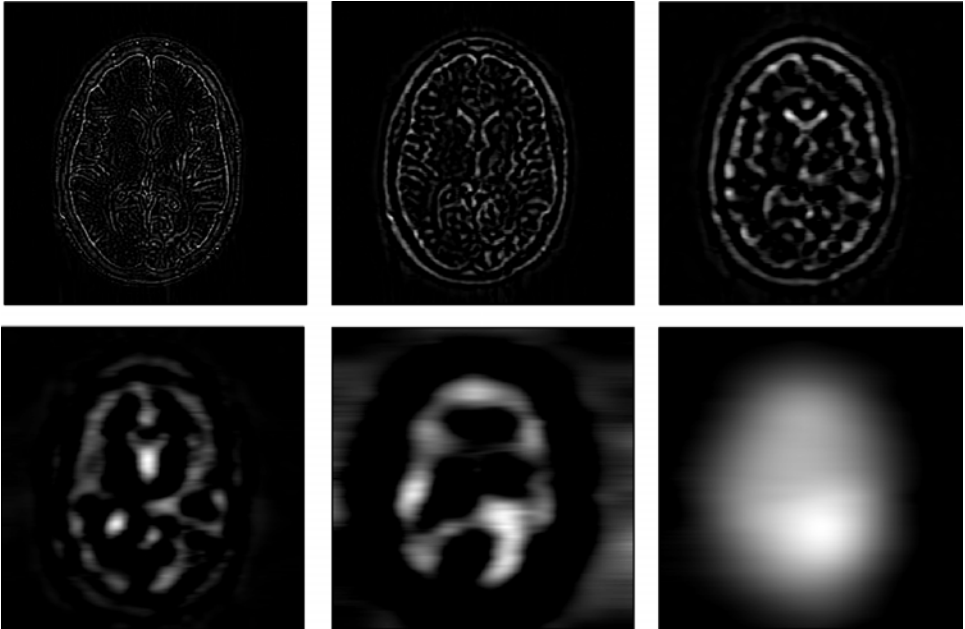


Fig. 15. The decomposition of the MR image. The upper panels are the n 2D IMF components for $n = 1, 2, 3$. The lower panels are components 4–6. This sequence represents image textural from finer to large scale.

anaplastic astrocytoma was found. A right frontal lesion was biopsied in 8/94. Recurrent tumor was suspected on the basis of the imaging, and was confirmed pathologically.”

The MR image is analyzed with the MEEMD. The results of the decomposition are given in Fig. 15.

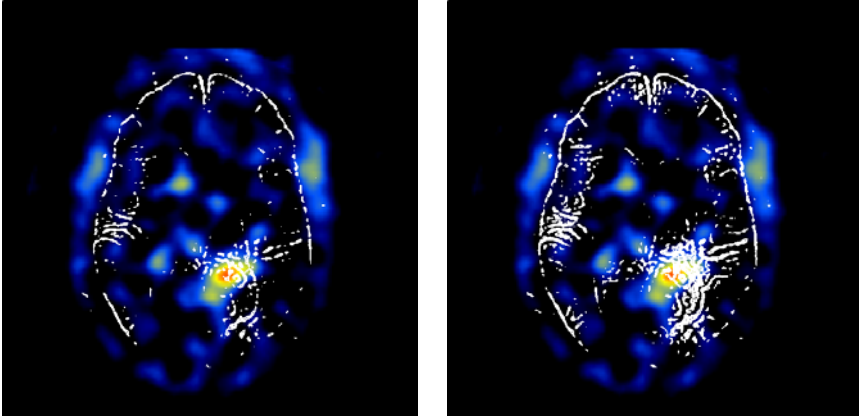


Fig. 16. The recombination from the decompositions of the MR image superposed on the Thallium SPECT image. These two panels are all from the combination of components 1 and 5, but with different contour selections: the left panel representing the contour starting from 1 to 30; the right one from 1 to 40. Note the concentrated contour areas near the tumor lesion.

In this present representation, the original image is decomposed into six components each representing a separate scale range. The first component represents the smallest scale or the finest textural, while the last one gives only the largest scale of the overall mean trend in intensity of the image. The various combinations of the individual components could be used to emphasize different textural and intensity variations of the image. As an example, the combination of the components 1 and 5 is used in the following images. This image accentuates the finest texture (component 1) and the intensity variation that still retained some structure of the original image (component 5). The combination is given in Fig. 16.

From Fig. 16, we can see that either contour presentation accentuates the region of the tumor lesion influence. Though the exact clinical implications need additional studies, the ability to accentuate selected area is potentially useful. In this case, the contour intensive area actually covers the whole abnormal region. For example, the contoured area may not represent the active tumor lesion, but the edematous brain tissue; the contours could enable us to quantify the lesion and the degree of severity of the tumor. Other combinations are possible, of course. The present example gives only an indication for potential future applications of the decomposed results.

6. Conclusion

In this paper, we developed a multi-dimensional ensemble EMD method, designated as MEEMD, for image and other higher-dimensional data analysis. The method is based on a completely different approach from those serving as the foundations for traditional 2D EMD methods. The new method bypasses major obstacles and difficulties in defining extrema, in obtaining membrane fitting. Significant improvements

also include the elimination of scale mixing and thereby the decomposed results should contain no artificial structures.

The MEEMD can be easily extended to spatially three or more dimensional fields without any barrier. Such extension would not be feasible for the traditional two-dimensional approach, for the method to fit the spatially scattered data in higher dimension would involve membrane of higher manifold would soon lose direct geometrical meaning and the computations, even if possible, would be prohibitively expensive. The present slice approach could still be clearly and systematically implemented. Furthermore, the equivalence of higher order saddle points, ridges, and valleys would not be a problem in the present approach. With the EEMD added, the problems of mode mixing would not be a problem. To overcome all these problems in the traditional approach would be an insurmountable task. Finally, the slice approach had reduced the data into one-dimensional data strings; then, one could easily use the Hilbert transform to compute the wave number spectra as a different representation of the spatial features. Such a different view in the wave number space would not have its counter part in the traditional DEMD.

Acknowledgments

This research was completed while ZW and XYC were visiting professors at NCU supported by grants from NSC, NSC95-2119-M-008-031-MY3, NSC97-2627-B-008-007, and finally a grant from NCU 965941. N. E. Huang was supported by a grant from Federal Highway Administration, DTFH61-08-00028, and the same grants from NSC, NSC95-2119-M-008-031-MY3, NSC97-2627-B-008-007, and finally a grant from NCU 965941 that have made the conclusion of this study possible. He is also supported by a TSMC endowed chair at NCU.

Appendix. Program

A patent has been filed for the method by the National Central University in both the US and Taiwan.

A Matlab program for decomposition of image “Lena” is provided to illustrate how the newly proposed method works. It should be noted here that the reason we display the Matlab program instead of the programs using some other major computational programming languages, such as C, C++, Fortran, etc., is that Matlab is more a scripting computational language that can illustrate the idea in more concise and clear fashion. The implementation, however, is not limited to Matlab program, of course. MEEMD could be easily implemented in any computational language. This and many other programs, related to Hilbert–Huang transform, could also be found in and freely downloaded from the Website of Research Center for Adaptive Data Analysis, National Central University, Chungli, Taiwan at: <http://www.ncu.edu.tw/~ncu34951/>.

The program is designed according to the following schematics:

Schematics

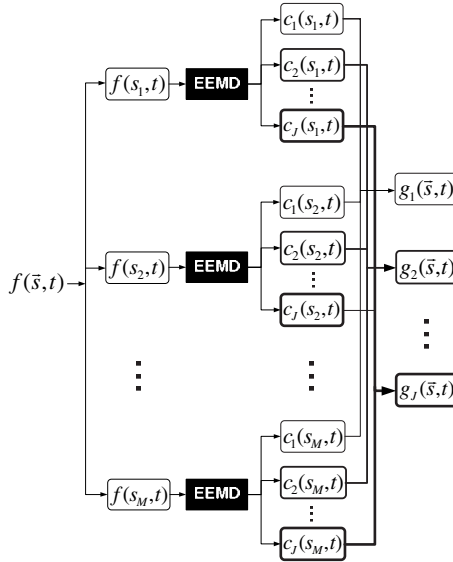


Fig. s1. Spatial-temporal multi-dimensional EMD based on EEMD.

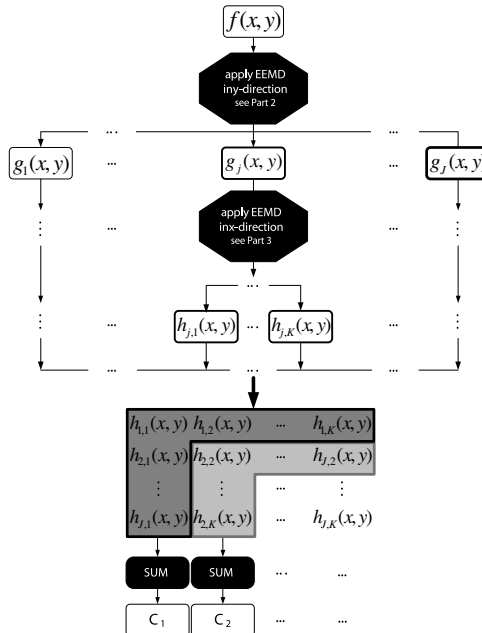


Fig. s2(a). Spatial two-dimensional EMD based on EEMD, part 1: overview.

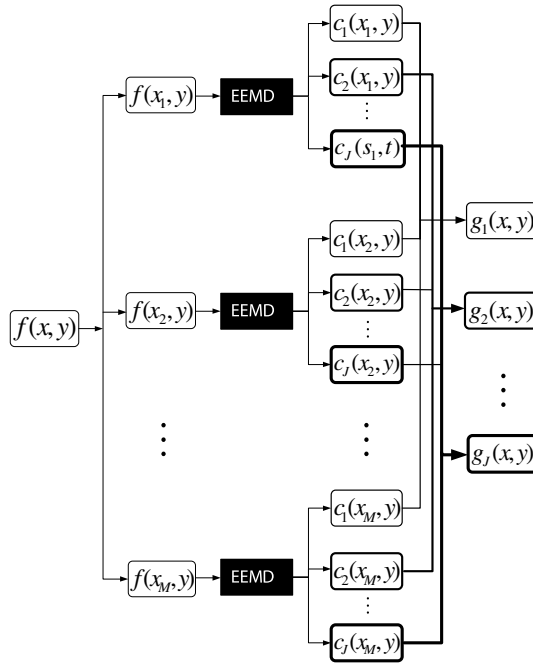


Fig. s2(b). Spatial two-dimensional EMD based on EEMD, part 2: decomposition in the first direction.

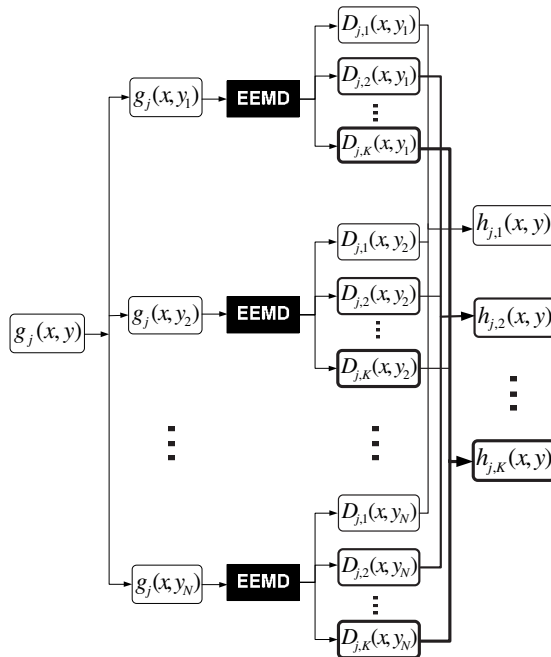


Fig. s2(c). Spatial two-dimensional EMD based on EEMD, part 3: decomposition in the second direction.

The program modules including the following files:

1. driver: *lenadecomp.m*

```

clear;
clf;

% loading image data
load lena2.dat;

% image data size in one-dimension
N=111;

% specify ensemble number
nesb=100;

% decomposition in the first dimension and arrange the output
for i=1:N,
    temp=lena2(i,:);
    rslt=eemd(temp,0.2,nesb,4);
    for j=1:N,
        for k=1:5,
            rsltd1(i,j,k)=rslt(j,k+1);
        end
    end
end

% decomposition in the second direction
for k=1:5,
    for j=1:N,
        temp2=rsltd1(:,j,k);
        rslt=eemd(temp2,0.2,nesb,4);
        for i=1:N,
            for kk=1:5,
                rslt2d(i,j,k,kk)=rslt(i,kk+1);
            end
        end
    end
end

% combine modes
for i=1:N
    for j=1:N,

```

```

        for m=1:5,
            rsltf(i,j,m)=0;
            for k=m:5,
                rsltf(i,j,m)=rsltf(i,j,m)+rslt2d(i,j,k,m);
                rsltf(i,j,m)=rsltf(i,j,m)+rslt2d(i,j,m,k);
            end
            rsltf(i,j,m)=rsltf(i,j,m)-rslt2d(i,j,m,m);
        end
    end
end
end
end

```

2. function 1: *eemd.m*

```

% Y: Inputted data;
% Nstd: ratio of the standard deviation of the added noise and that
of Y;
% NE: Ensemble member being used
% TNM: total number of modes (not including the trend)
%

```

```
function allmode=eemd(Y,Nstd,NE,TNM)
```

```

% find data length
xsize=length(Y);
dd=1:1:xsize;

% Normaliz data
Ystd=std(Y);
Y=Y/Ystd;

% Initialize saved data
TNM2=TNM+2;
for kk=1:1:TNM2,
    for ii=1:1:xsize,
        allmode(ii,kk)=0.0;
    end
end

for iii=1:1:NE,
% adding noise
    for i=1:xsize,
        temp=randn(1,1)*Nstd;
        X1(i)=Y(i)+temp;
    end
end

```

```

    X2(i)=Y(i)-temp;
end

% sifting X1
xorigin = X1;
xend = xorigin;

% save the initial data into the first column
for jj=1:1:xsize,
    mode(jj,1) = xorigin(jj);
end

nmode = 1;
while nmode <= TNM,
    xstart = xend;
    iter = 1;

    while iter<=10,
        [spmax, spmin, flag]=extrema(xstart);
        upper= spline(spmax(:,1),spmax(:,2),dd);
        lower= spline(spmin(:,1),spmin(:,2),dd);
        mean_ul = (upper + lower)/2;
        xstart = xstart - mean_ul;
        iter = iter +1;
    end
    xend = xend - xstart;

    nmode=nmode+1;

    % save a mode
    for jj=1:1:xsize,
        mode(jj,nmode) = xstart(jj);
    end
end

% save the trend
for jj=1:1:xsize,
    mode(jj,nmode+1)=xend(jj);
end

% add mode to the sum of modes from earlier ensemble members
allmode=allmode+mode;

```

```

%%%======
% sifting X2
xorigin = X2;
xend = xorigin;

% save the initial data into the first column
for jj=1:1:xsize,
    mode(jj,1) = xorigin(jj);
end

nmode = 1;
while nmode <= TNM,
    xstart = xend;
    iter = 1;

    while iter<=10,
        [spmax, spmin, flag]=extrema(xstart);
        upper= spline(spmax(:,1),spmax(:,2),dd);
        lower= spline(spmin(:,1),spmin(:,2),dd);
        mean_ul = (upper + lower)/2;
        xstart = xstart - mean_ul;
        iter = iter +1;
    end
    xend = xend - xstart;

    nmode=nmode+1;

    % save a mode
    for jj=1:1:xsize,
        mode(jj,nmode) = xstart(jj);
    end
end

% save the trend
for jj=1:1:xsize,
    mode(jj,nmode+1)=xend(jj);
end

% add mode to the sum of modes from earlier ensemble members
allmode=allmode+mode;
end

```

```

% ensemble average
allmode=allmode/NE/2;

% Rescale mode to original unit.
allmode=allmode*Ystd;

3. function: extrema.m

% This is function to find all the extrema

function [spmax, spmin, flag]= extrema(in_data)

flag=1;
dsize=length(in_data);

% find all the maximums
spmax(1,1) = 1;
spmax(1,2) = in_data(1);
jj=2;
kk=2;
while jj<dsize,
    if ( in_data(jj-1)<=in_data(jj) & in_data(jj)>=in_data(jj+1) )
        spmax(kk,1) = jj;
        spmax(kk,2) = in_data (jj);
        kk = kk+1;
    end
    jj=jj+1;
end
spmax(kk,1)=dsize;
spmax(kk,2)=in_data(dsize);

if kk>=4
    slope1=(spmax(2,2)-spmax(3,2))/(spmax(2,1)-spmax(3,1));
    tmp1=slope1*(spmax(1,1)-spmax(2,1))+spmax(2,2);
    if tmp1>spmax(1,2)
        spmax(1,2)=tmp1;
    end

    slope2=(spmax(kk-1,2)-spmax(kk-2,2))/(spmax(kk-1,1)-spmax(kk-2,1));
    tmp2=slope2*(spmax(kk,1)-spmax(kk-1,1))+spmax(kk-1,2);
    if tmp2>spmax(kk,2)
        spmax(kk,2)=tmp2;
    end
end

```

```

else
    flag=-1;
end

msize=size(in_data);
dsize=max(msize);
xsize=dsize/3;
xsize2=2*xsize;

spmin(1,1) = 1;
spmin(1,2) = in_data(1);
jj=2;
kk=2;
while jj<dsize,
    if ( in_data(jj-1)>=in_data(jj) & in_data(jj)<=in_data(jj+1))
        spmin(kk,1) = jj;
        spmin(kk,2) = in_data (jj);
        kk = kk+1;
    end
    jj=jj+1;
end
spmin(kk,1)=dsize;
spmin(kk,2)=in_data(dsize);

if kk>=4
    slope1=(spmin(2,2)-spmin(3,2))/(spmin(2,1)-spmin(3,1));
    tmp1=slope1*(spmin(1,1)-spmin(2,1))+spmin(2,2);
    if tmp1<spmin(1,2)
        spmin(1,2)=tmp1;
    end

    slope2=(spmin(kk-1,2)-spmin(kk-2,2))/(spmin(kk-1,1)-spmin(kk-2,1));
    tmp2=slope2*(spmin(kk,1)-spmin(kk-1,1))+spmin(kk-1,2);
    if tmp2<spmin(kk,2)
        spmin(kk,2)=tmp2;
    end
else
    flag=-1;
end

flag=1;

```

References

1. N. E. Huang, Computer implemented empirical mode decomposition apparatus, method and article of manufacture. US Patent 5,983,162, Granted Nov. 9, 1999.
2. N. E. Huang, Computer implemented empirical mode decomposition apparatus, method and article of manufacture for two-dimensional signals. US Patent 6,311,130 B1, Granted Oct. 30, 2001.
3. N. E. Huang, Empirical mode decomposition apparatus, method and article of manufacture for analyzing biological signals and performing curve fitting. US Patent 6,381,559 B1, Granted Apr. 30, 2002.
4. N. E. Huang, Empirical mode decomposition apparatus, method and article of manufacture for analyzing biological signals and performing curve fitting. US Patent 6,738,734 B1, Granted May 18, 2004.
5. Z. Wu and N. E. Huang, Noise assisted data analysis method, system and program product therefore, US20080065337A1, Granted March 13, 2008.
6. D. Gabor, Theory of communication, *J. IEE* **93** (1946) 426–457.
7. E. Bedrosian, On the quadrature approximation to the Hilbert transform of modulated signals, *Proc. IEEE* **51** (1963) 868–869.
8. A. H. Nuttall, On the quadrature approximation to the Hilbert transform of modulated signals, *Proc. IEEE* **54** (1966) 1458–1459.
9. N. E. Huang, Z. Shen, S. R. Long, M. C. Wu, E. H. Shih, Q. Zheng, C. C. Tung and H. H. Liu, The empirical mode decomposition and the Hilbert spectrum for nonlinear and non-stationary time series analysis, *Proc. Roy. Soc. London A* **454** (1998) 903–993.
10. N. E. Huang, Z. Wu, S. R. Long, K. C. Arnold, X. Chen and K. Blank, On instantaneous frequency, *Adv. Adapt. Data Anal.* **1** (2009) 177–229.
11. N. E. Huang, S. R. Long and Z. Shen, Frequency downshift in nonlinear water wave evolution, *Adv. Appl. Mech.* **32** (1996) 59–117.
12. N. E. Huang, Z. Shen and S. R. Long, A new view of nonlinear water waves — The Hilbert spectrum, *Ann. Rev. Fluid Mech.* **31** (1999) 417–457.
13. N. E. Huang, M. L. Wu, S. R. Long, S. S. Shen, W. D. Qu, P. Gloersen and K. L. Fan, A confidence limit for the empirical mode decomposition and Hilbert spectral analysis, *Proc. Roy. Soc. London A* **459** (2003) 2317–2345.
14. Z. Wu and N. E. Huang, A study of the characteristics of white noise using the empirical mode decomposition method, *Proc. Roy. Soc. London A* **460** (2004) 1597–1611.
15. Z. Wu and N. E. Huang, Statistical significance test of intrinsic mode functions, pp. 107–127, *Hilbert–Huang Transform and Its Applications*, eds. N. E. Huang and S. S. P. Shen (World Scientific, Singapore, 2005), 311 pp.
16. Z. Wu and N. E. Huang, Ensemble empirical mode decomposition: A noise-assisted data analysis method, *Adv. Adapt. Data Anal.* **1** (2009) 1–41.
17. Z. Wu, N. E. Huang, S. R. Long and C.-K. Peng, On the trend, detrending, and the variability of nonlinear and non-stationary time series, *Proc. Natl. Acad. Sci. USA* **104** (2007) 14889–14894.
18. Z. Wu, E. K. Schneider, B. P. Kirtman, E. S. Sarachik, N. E. Huang and C. J. Tucker, Amplitude-frequency modulated annual cycle: An alternative reference frame for climate anomaly, *Climate Dynam.* **31** (2008) 823–841.
19. N. E. Huang and N. O. Attoh-Okine (eds.), *Hilbert–Huang Transforms in Engineering* (CRC Taylor and Francis Group, 2005), 313 pp.
20. N. E. Huang and S. S. P. Shen (eds.), *Hilbert–Huang Transform and Its Applications* (World Scientific, Singapore, 2005), 311 pp.

21. N. E. Huang and Z. Wu, A review on Hilbert–Huang transform: Method and its applications to geophysical studies, *Rev. Geophys.* **46** (2008) RG2006, doi:10.1029/2007RG000228.
22. P. Flandrin, G. Rilling and P. Gonçalves, Empirical mode decomposition as a filter-bank, *IEEE Sig. Process. Lett.* **11** (2004) 112–114.
23. P. Flandrin, P. Gonçalves and G. Rilling, EMD equivalent filter banks from interpretation to applications, pp. 57–74, in *Hilbert–Huang Transform and Its Applications*, eds. N. E. Huang and S. S. P. Shen (World Scientific, Singapore, 2005), 311 pp.
24. P. Flandrin and P. Gonçalves, Empirical mode decompositions as data-driven wavelet-like expressions, *Int. J. Wavelet Multiresolut. Inform. Process.* **2** (2004) 469–477.
25. S. R. Long, Applications of HHT in image analysis, pp. 289–305, *Hilbert–Huang Transform and Its Applications*, eds. N. E. Huang and S. S. P. Shen (World Scientific, Singapore, 2005), 311 pp.
26. J. C. Nunes, Y. Bouaoune, E. Delechelle, O. Niang and P. Bunel, Image analysis by bidimensional empirical mode decomposition, *Image Vision Comput.* **21** (2003) 1019–1026.
27. J. C. Nunes, O. Niang, Y. Bouaoune, E. Delechelle and P. Bunel, Bidimensional empirical mode decomposition modified for texture analysis, *Image Anal. Proc.* **2749** (2003) 171–177.
28. J. C. Nunes, S. Guyot and E. Delechelle, Texture analysis based on local analysis of the bidimensional empirical mode decomposition, *Machine Vision Appl.* **16** (2005) 177–188.
29. A. Linderhed, Variable sampling of the empirical mode decomposition of two-dimensional signals, *Int. J. Wavelets Multiresolution Inform. Process.* **3** (2005) 435–452.
30. A. Linderhed, Image empirical mode decomposition: A new tool for image processing, *Adv. Adapt. Data Anal.* **1** (2009) 265–294.
31. P. Song and J. Zhang, On the application of two-dimensional empirical mode decomposition in the information separation of oceanic remote sensing image, *High Technol. Lett.* **11** (2001) 62–67 (in Chinese).
32. C. Damerval, S. Meignen and V. Perrier, A fast algorithm for bidimensional EMD, *IEEE Sig. Process. Lett.* **12** (2005) 701–704.
33. Y. Yuan, M. Jin, P. Song and J. Zhang, Empirical and dynamical detection of the sea bottom topography from synthetic aperture radar image. *Adv. Adapt. Data Anal.* **1** (2009) 243–263.
34. Y. Xu, B. Liu, J. Liu and S. Riemenschneider, Two-dimensional empirical mode decomposition by finite elements, *Proc. Roy. Soc. London A* **462** (2006) 3081–3096.
35. S. M. A. Bhuiyan, N. O. Attoh-Okine, K. E. Barner, A. Y. Ayenu and R. R. Adhami, Bidimensional empirical mode decomposition using various interpolation techniques, *Adv. Adapt. Data Anal.* **1** (2009) 309–338.
36. N. A. Rayner, D. E. Parker, E. B. Horton, C. K. Folland, L. V. Alexander, D. P. Rowell, E. C. Kent and A. Kaplan, Global analyses of sea surface temperature, sea ice, and night marine air temperature since the late nineteenth century, *J. Geophys. Res.* **108**(D14) (2003) 4407, doi:10.1029/2002JD002670.
37. N. E. Huang, H. H. Shih, Z. Shen, S. R. Long and K. L. Fan, The ages of large amplitude coastal seiches on the Caribbean Coast of Puerto Rico, *J. Phys. Oceanogr.* **30** (2000) 2001–2012.